



**Reconstruction of seasonal temperature variability in the tropical Pacific Ocean from the shell  
of the scallop, *Comptopallium radula***

**JULIEN THÉBAULT,<sup>1,\*</sup> LAURENT CHAUVAUD,<sup>2</sup> JACQUES CLAVIER,<sup>2</sup> JENNIFER GUARINI,<sup>3</sup>  
ROBERT B. DUNBAR,<sup>4</sup> RENAUD FICHEZ,<sup>5</sup> DAVID A. MUCCIARONE,<sup>4</sup> and ERIC MORIZE<sup>6</sup>**

(1) IRD, Unité de Recherche Camélia, BP A5, 98848 Nouméa Cedex, New Caledonia

(2) IUEM-UBO, UMR CNRS 6539, Place Nicolas Copernic, 29280 Plouzané, France

(3) Observatoire Océanologique de Banyuls, Université Pierre et Marie Curie, UMR CNRS 7621,  
66650 Banyuls-sur-Mer, France

(4) Department of Geological and Environmental Sciences, Stanford University, Stanford, CA 94305-  
2115, USA

(5) Centre d'Océanologie de Marseille, Station Marine d'Endoume, Rue de la Batterie des Lions,  
13007 Marseille, France

(6) Centre IRD de Bretagne, US Chronos, BP 70, 29280 Plouzané, France

Running head: Scallop shells as temperature recorders in the Pacific Ocean

\* Corresponding author. Present address: IUEM-UBO, UMR CNRS 6539, Place Nicolas Copernic,  
29280 Plouzané, France. *E-mail:* [julien.thebault@univ-brest.fr](mailto:julien.thebault@univ-brest.fr)

1  
2  
3  
4  
5  
6  
7  
8  
9  
10  
11  
12  
13  
14  
15  
16  
17  
18  
19  
20  
21  
22  
23  
24  
25  
26  
**ABSTRACT**

We investigated the oxygen isotope composition ( $\delta^{18}\text{O}$ ) of shell striae from juvenile *Comptopallium radula* (Mollusca; Pectinidae) specimens collected live in New Caledonia. Bottom-water temperature and salinity were monitored in-situ throughout the study period. External shell striae form with a 2-day periodicity in this scallop, making it possible to estimate the date of precipitation for each calcite sample collected along a growth transect. The oxygen isotope composition of shell calcite ( $\delta^{18}\text{O}_{\text{shell calcite}}$ ) measured at almost weekly resolution on calcite accreted between August 2002 and July 2003 accurately tracks bottom-water temperatures. A new empirical paleotemperature equation for this scallop species relates temperature and  $\delta^{18}\text{O}_{\text{shell calcite}}$ :

$$t(^{\circ}\text{C}) = 20.00(\pm 0.61) - 3.66(\pm 0.39) \times (\delta^{18}\text{O}_{\text{shell calcite VPDB}} - \delta^{18}\text{O}_{\text{water VSMOW}})$$

The mean absolute accuracy of temperature estimated using this equation is 1.0 °C at temperatures between 20 and 30 °C. Uncertainties regarding the precise timing of  $\text{CaCO}_3$  deposition and the actual variations in  $\delta^{18}\text{O}_{\text{water}}$  at our study sites probably contribute to this error. Comparison with a previously published empirical paleotemperature equation indicates that *C. radula* calcite is enriched in  $^{18}\text{O}$  by  $\sim 0.7$  ‰ relative to equilibrium. Given the direction of this offset and the lack of correlation between shell growth rate and  $\delta^{18}\text{O}_{\text{shell calcite}}$ , this disequilibrium is unlikely to be related to kinetic isotope effects. We suggest that this enrichment reflects (1) a relatively low pH in the scallop's marginal extrapallial fluid (EPF), (2) an isotopic signature of the EPF different from that of seawater, or (3) Rayleigh fractionation during the biocalcification process. Relative changes in  $\delta^{18}\text{O}_{\text{shell calcite}}$  reflect seawater temperature variability at this location and we suggest that the shell of *C. radula* may be useful as an archive of past seawater temperatures.

27

## 1. INTRODUCTION

28

29 Paleoclimate archives are important tools for understanding the causes of climate change  
30 and for the validation of climate models (Dunbar and Cole, 1999). In most climate models, sea  
31 surface temperature (SST) is an important variable because of its correlation with and control of  
32 other climate parameters such as atmospheric moisture content and temperature, rainfall, and  
33 heat flux. The known spatial heterogeneity of climatic response to changes in radiative forcing  
34 suggests a need for well-calibrated paleoclimate records from diverse geographic settings.

35 The oxygen isotope ratio ( $^{18}\text{O}/^{16}\text{O}$ ) of marine biogenic carbonate is controlled by  
36 temperature and the oxygen isotope composition of the seawater from which it precipitates  
37 (McCrea, 1950; Epstein et al., 1953). Oxygen isotope paleothermometry has been employed in a  
38 number of studies of Cenozoic marine molluscs (Krantz et al., 1987; Andreasson and Schmitz,  
39 1996; Bice et al., 1996; Andreasson and Schmitz, 1998; Kirby et al., 1998; Andreasson and  
40 Schmitz, 2000; Hickson et al., 2000; Tripathi et al., 2001; Dutton et al., 2002) because their shells  
41 grow by periodic accretion of calcite or aragonite (Pannela and McClintock, 1968). This  
42 characteristic provides a means of assigning calendar dates to each successive band of accreted  
43 shell material, assuming that the periodicity of accretion is known. Using improved micro-  
44 sampling and micro-analytical techniques, several recent studies have demonstrated that rapidly  
45 growing bivalve mollusc shells contain high resolution proxy records of seawater temperature  
46 (Kennedy et al., 2001; Elliot et al., 2003; Chauvaud et al., 2005).

47 In this study, we compare in-situ instrumental seawater temperature with the oxygen  
48 isotope composition of shell calcite from six juvenile scallops (*Comptopallium radula*, L., 1758)  
49 from the southwest lagoon of New Caledonia (Fig. 1a). *C. radula* is a large ( $H_{\infty} = 92.4$  mm;  
50 Lefort, 1994) sedentary scallop that lives under branching corals or on coralline fragment beds,  
51 generally between 0.5 and 5 m depth, in the tropical Indo-West Pacific Ocean. As in many other  
52 scallop species, the shell surface of *C. radula* is textured with concentric striae (Fig. 1b).  
53 Marking experiments using calcein fluorescent dye have demonstrated that one stria is formed  
54 every two days (Thébault et al., 2006). We have now measured the oxygen isotope composition

55 of carbonate samples collected along shell growth transects to develop an empirical temperature  
56 equation which is then compared with some previous  $\delta^{18}\text{O}$ :temperature relationships calibrated  
57 for inorganically precipitated calcite and other molluscs.

58 Most previous paleotemperature records from this region are derived from elemental and  
59 isotopic ratios in scleractinian corals (Beck et al., 1992; Quinn et al., 1996a,b; Quinn et al.,  
60 1998; Quinn and Sampson, 2002; Watanabe et al., 2003; Corrège et al., 2004; Kilbourne et al.,  
61 2004). Our dataset contributes to the relatively small number of oxygen isotope studies on  
62 scallop species (Krantz et al., 1984; Krantz et al., 1987; Tan et al., 1988; Hickson et al., 2000;  
63 Owen et al., 2002a,b; Chauvaud et al., 2005) and allows the evaluation of the potential of *C.*  
64 *radula* for paleoclimatic studies.

65

66

## 2. METHODS

67

### 2.1. Study area

69

70 New Caledonia is located in the southwest Pacific Ocean, between 19-23°S and  
71 163-168°E (Fig. 2). The main island, Grande Terre, is surrounded by an 1100 km long barrier  
72 reef. The southwest lagoon covers 2066 km<sup>2</sup> and has an average depth of 21 m. Our study sites  
73 near Nouméa are Sainte-Marie Bay (22°18'22"S, 166°28'89"E) and Koutio Bay (22°13'45"S,  
74 166°25'33"E). Both sites are shallow (< 5 m depth) with muddy sandy sediment. Bottom-water  
75 temperatures and salinities were measured from August 7, 2002 to August 1, 2003.  
76 Temperatures were recorded hourly using a EBRO EBI-85A thermal probe fixed to a bottom  
77 mooring (accuracy  $\pm 0.1$  °C). Salinity (average of the first meter of the water column above the  
78 seafloor) was measured weekly using a SeaBird SBE19 CTD profiler, and is reported using the  
79 Practical Salinity Scale. Salinity data were interpolated linearly to obtain daily values.

80 Because salinity and  $\delta^{18}\text{O}_{\text{water}}$  are positively correlated (Craig and Gordon, 1965), the  
81 oxygen isotope composition of water was measured at twelve sampling sites along a salinity  
82 gradient in the Dumbéa River (Fig. 2) at the beginning of the 2003 dry season (normal river

83 flow). The  $\delta^{18}\text{O}_{\text{water}}$  analyses were performed using a modification of the standard  $\text{CO}_2\text{-H}_2\text{O }^{18}\text{O}$   
84 isotope equilibration technique (Epstein and Mayeda, 1953). For each sample, 2.4 mL of water  
85 were equilibrated for 6 h in a reaction vessel with  $\text{CO}_2$  at 880 mbar and 21 °C. A cold trap at  
86 -80 °C was used to remove water and the resultant  $\text{CO}_2$  was frozen onto a cold finger prior to  
87 analysis on a Europa SIRA II dual-inlet isotope ratio mass spectrometer. The internal standard  
88 used was North Sea Water ( $\delta^{18}\text{O} = -0.20 \text{‰}$  VSMOW). Analytical precision was 0.06 ‰ (1 $\sigma$ ).  
89 All samples were run in duplicate and data are reported in ‰ with respect to VSMOW. Salinity  
90 was measured using a Guildline 8410A Portasal inductive salinometer (accuracy  $\pm 0.002$ ),  
91 calibrated with IAPSO Standard Seawater (Ocean Scientific International Ltd., Petersfield, UK).  
92 Three samples were measured in triplicate with an average standard deviation of 0.008.

93

## 94 2.2. Scallop sampling, preparation, and analysis

95

96 *Comptopallium radula* grows rapidly, especially during the first two years of life (Lefort,  
97 1994). After sexual maturity is achieved during the third year (Lefort and Clavier, 1994), the  
98 annual shell growth rate drops. For this study only juvenile scallops were analysed because they  
99 have the largest annual increase in shell size (compared with mature specimens) and provide the  
100 highest temporal resolution in carbonate records.

101 Six live juvenile *C. radula* specimens (maximum shell height = 69.2 mm) were collected  
102 by SCUBA diving at the beginning of the 2003 cool season. In Sainte-Marie Bay, shell SM1  
103 was collected on June 23, shell SM2 on July 1, and shell SM3 on July 13. In Koutio Bay, shell  
104 BK1 was harvested on May 21, shell BK2 on June 14, and shell BK3 on July 2. After  
105 collection, the scallops were immediately killed and their shells cleaned by soaking in 90 %  
106 acetic acid for 45-60 s to remove bio-fouling, and then rinsed with distilled water and air-dried.

107 Shell samples ( $n = 225$ ; 34 to 40 samples per shell) for isotopic analyses were collected  
108 (using a hand-held micro-drill equipped with a 0.6-mm engraving bit) along a transect line  
109 perpendicular to the striae, from the umbo to the ventral margin (Fig. 1b). Drilling was  
110 restricted to the ridges of the striae to ensure that shell material was not cross-contaminated by

111 mineralogically different layers of CaCO<sub>3</sub>. Because the distance between two successive striae  
112 is not constant, each sample contained material from 2 to 5 striae (average = 2.3 striae/sample),  
113 and was separated from the next sample by 1 to 3 striae (average = 1.2 striae). Given the 2-day  
114 periodicity of striae formation (Thébault et al., 2006), this sampling scheme means that each  
115 sample corresponds approximately to 7 days of growth.

116 Aliquots of shell calcite weighing between 32 and 212 µg (mean = 88 µg) were acidified  
117 in 100 % phosphoric acid at 70 °C for 470 s and analyzed using an automated Finnigan MAT  
118 Kiel III carbonate device coupled to a Finnigan MAT 252 isotope ratio mass spectrometer at  
119 Stanford University. Shell isotopic data are expressed in conventional delta (δ) notation (Epstein  
120 et al., 1953) relative to the VPDB standard. A total of 25 samples of the international isotopic  
121 reference standard NBS-19 (mean weight of standard aliquots = 83 µg) and 15 samples of the  
122 Stanford Isotope Lab Standard SLS-1 (mean weight = 84 µg) were analyzed with the scallops  
123 and yielded a reproducibility (1σ) of 0.049 ‰ VPDB (NBS-19) and 0.051 ‰ VPDB (SLS-1)  
124 for δ<sup>18</sup>O, and 0.029 ‰ VPDB (NBS-19) and 0.035 ‰ VPDB (SLS-1) for δ<sup>13</sup>C.

125 A date of formation was assigned to each sample drilled from all shells (except SM2) by  
126 backdating from the outer most stria (i.e., harvest date), based on the 2-day periodicity of striae  
127 formation in juvenile *C. radula* (Thébault et al., 2006). A different method was used for shell  
128 SM2 because of a clearly visible hiatus in shell growth on its external surface. This growth  
129 hiatus corresponds to a period during which shell growth ceased. The date of growth cessation  
130 and the duration of the interval of zero growth were, however, unknown. The method we used  
131 for shell SM2 is based on the very small inter-individual variability of δ<sup>18</sup>O<sub>shell calcite</sub> profiles in *C.*  
132 *radula*. First, all samples collected between the ventral margin and the growth hiatus were dated  
133 using the method described for the 5 other shells (time-anchored part of the SM2 δ<sup>18</sup>O profile -  
134 absolute chronology). Then, each sample collected between the growth hiatus and the umbo was  
135 dated in relation to the next one, based on the periodicity of striae formation (time-unanchored  
136 part of the SM2 δ<sup>18</sup>O profile - relative chronology). Finally, this time-unanchored part of the  
137 SM2 δ<sup>18</sup>O profile was time correlated with the mean δ<sup>18</sup>O profile calculated from the other 5

138 shells, allowing us to determine the absolute chronology of the dataset (synchronization  
139 involved the maximization of the correlation coefficient between these two datasets). This  
140 method permits the estimation of the date of growth cessation as well as the duration of the  
141 interval of zero growth.

142 An estimate of shell growth rate, based on the periodicity of striae formation, was made  
143 for each shell by measuring distances between successive striae (growth increment width) using  
144 an image analysis technique described in detail by Chauvaud et al. (1998). The estimated  
145 growth rates are expressed in  $\mu\text{m } 2\text{d}^{-1}$ . In this paper, we define “shell growth rate” as the  
146 dorso-ventral linear extension of the shell per unit time. Since this does not take into account  
147 ontogenetic changes in shell thickness, growth rate is likely to differ from absolute calcification  
148 rate (see Gillikin et al. (2005) for a helpful discussion).

149 The outer layer of scallop shells was found to be composed of pure foliated calcite (Roux  
150 et al., 1990; Barbin et al., 1991). Nevertheless, we checked the mineralogy of the striae we  
151 sampled using an X-ray powder diffractometer equipped with an INEL curved  
152 position-sensitive detector (CPS120) and a graphite monochromator, using  $\text{CoK}_{\alpha 1}$  radiation at  
153 35 mA and 30 kV.

154

### 155 **2.3. Calibration of the $\delta^{18}\text{O}$ :temperature relationship**

156

157 As described in section 2.2, the  $\delta^{18}\text{O}$  value of each sample represents an average of  
158  $\sim 5$  days growth ( $\sim 2.3$  striae). To match this isotopic time averaging, 5-day moving averages of  
159 temperature and interpolated weekly salinity measurements were calculated for the calibration.  
160 Ordinary Least Squares (OLS) regression was used to examine the  $\delta^{18}\text{O}$ :temperature  
161 relationship, by expressing  $\delta^{18}\text{O}$  as the isotopic difference between shell calcite and seawater:

162

$$163 \quad t = A + B \times (\delta^{18}\text{O}_{\text{shell calcite}} - \delta^{18}\text{O}_{\text{water}}), \quad (1)$$

164

165 where  $t$  is temperature ( $^{\circ}\text{C}$ ),  $A$  and  $B$  are constants, and  $\delta^{18}\text{O}_{\text{shell calcite}}$  and  $\delta^{18}\text{O}_{\text{water}}$  are expressed  
166 in ‰ relative to VPDB and VSMOW, respectively. A “comparison of regression lines”  
167 procedure (Statgraphics Centurion XV statistical software) was used to test whether there were  
168 significant differences between the slopes of the OLS regressions calculated for each of the six  
169 shells, and between the slopes of the OLS regressions calculated for each of the two study sites.

170 This relationship was then compared to previous paleotemperature equations established  
171 for other calcitic molluscs (Epstein et al., 1953; Owen et al., 2002a; Chauvaud et al., 2005) and  
172 for inorganically precipitated calcite (Kim and O'Neil, 1997). In the equation of Epstein et al.  
173 (1953), later modified by Craig (1965), both calcite and water oxygen isotope data are relative  
174 to the same working standard of the mass spectrometer used in the early days at the University  
175 of Chicago, i.e.,  $\text{CO}_2$  from PDB. Water analyses normalized to the VSMOW scale and  
176 carbonates normalized to the VPDB scale cannot be used in this equation. However, it was  
177 rewritten by Sharp (2006) in a form appropriate for calcite and water oxygen isotope data  
178 expressed relative to VPDB and VSMOW, respectively. The equation of Owen et al. (2002a)  
179 was also rewritten in a form suitable for comparison, considering the whole of their dataset (i.e.,  
180 31 data points instead of 22 in their equation). To allow comparison with our linear relationship,  
181 the equation of Kim and O'Neil (1997) was modified from the form  $10^3 \ln \alpha = A(10^3 T^{-1}) + B$ ,  
182 and was approximated by a least squares linear regression following conversion of their  
183  $\delta^{18}\text{O}_{\text{calcite}}$  data to the VPDB scale. Calcite oxygen isotope data reported on the VSMOW scale in  
184 their study were first corrected (+0.25 ‰) to account for differences between the acid  
185 fractionation factor they used (1.01050) and the one commonly accepted for the reaction of  
186 carbonate with  $\text{H}_3\text{PO}_4$  at  $25^{\circ}\text{C}$  (1.01025). These data were then converted to the VPDB scale  
187 using the equation of Coplen et al. (1983). The coefficients of these four paleotemperature  
188 equations are reported in Table 1.

189

190

### 3. RESULTS

191

#### 3.1. Hydrologic survey

193

194 From August 2002 to August 2003, the average daily bottom-water temperature ranged  
195 from 20.4 to 29.3 °C in Sainte-Marie Bay, and from 20.1 to 29.7 °C in Koutio Bay. The mean  
196 diurnal temperature range was 0.6 °C in Sainte-Marie Bay and 0.9 °C in Koutio Bay, with  
197 maximum amplitudes of 1.7 and 1.9 °C, respectively. Bottom-water salinity ranged from 34.73  
198 to 36.18 in Sainte-Marie Bay, and from 33.43 to 36.52 in Koutio Bay. The water oxygen isotope  
199 composition showed a linear co-variation with salinity over the range 2.33-34.68. The  
200 relationship between  $\delta^{18}\text{O}_{\text{water}}$  and salinity based on a least squares regression equation ( $n = 12$ ,  
201  $r^2 = 0.999$ ,  $p < 0.001$ ) was:

202

$$203 \quad \delta^{18}\text{O}_{\text{water VSMOW}} = 0.168(\pm 0.003) S - 5.068(\pm 0.08), \quad (2)$$

204

205 Quoted errors on the slope and intercept are the 95 % confidence intervals. Extrapolating this  
206 linear relationship to a salinity of 36.52 yields a  $\delta^{18}\text{O}_{\text{water}}$  annual range of 0.24 ‰ in Sainte-  
207 Marie Bay and 0.52 ‰ in Koutio Bay.

208

#### 209 3.2. Mineralogy, shell growth rate and $\delta^{18}\text{O}_{\text{shell calcite}}$

210

211 X-ray diffractograms obtained from powder samples of the shell of *C. radula*  
212 unambiguously indicated that striae are composed of calcite. Nevertheless, as XRD is a bulk  
213 detection method, we cannot unequivocally state that striae do not contain small amounts of  
214 aragonite or magnesium carbonate.

215

216

217

The oxygen isotope composition of shell calcite, shell growth rate estimates, and  
bottom-water temperature are superimposed for each shell in Fig. 3. For all specimens, except  
SM2, it was not possible to reconstruct growth curves for portions of the shells accreted before

218 August 2002 because of striae abrasion in the oldest parts of the shells. The average shell  
219 growth rate was  $263 \mu\text{m } 2\text{d}^{-1}$  with maximum values on the order of  $450 \mu\text{m } 2\text{d}^{-1}$ . There is little  
220 similarity between the six growth rate profiles, and no clear seasonal cycle of growth.  
221 Moreover, the isotopic record from shell SM2 indicates a growth stop for ca. 2.5 months during  
222 the Summer of 2002-2003.

223 The oxygen isotope composition of shell calcite ranged from -1.47 to 0.28 ‰ VPDB (Fig.  
224 3). Isotopic profiles of the six shells show similar variations in 2002-2003. In order to determine  
225 the influence of temperature, salinity and shell growth rate on  $\delta^{18}\text{O}_{\text{shell calcite}}$ , the  $\delta^{18}\text{O}$  data were  
226 fit to a multivariate model of these variables (Table 2). Considering that the  $p$ -value for shell  
227 growth rate was 0.365 (i.e.,  $p > 0.01$ ), this term was not statistically significant and the model  
228 was therefore simplified. The best multiple linear regression model incorporated only salinity  
229 and temperature. In this model, however, salinity explained only 0.46 % of the variation in  
230  $\delta^{18}\text{O}_{\text{shell calcite}}$ . Our model also revealed the existence of a statistically significant effect of the  
231 interaction "temperature\*salinity".  
232

### 233 3.3. Calibration of the paleotemperature equation

234

235 To develop a paleotemperature equation, we used *C. radula*  $\delta^{18}\text{O}_{\text{shell calcite}}$ , and 5-day  
236 moving averages of daily temperature and  $\delta^{18}\text{O}_{\text{water}}$  (calculated from salinity measurements). The  
237 resulting linear relationship ( $n = 225$ ,  $r^2 = 0.609$ ,  $p < 0.001$ , Fig. 4) is:

238

$$239 \quad t(^{\circ}\text{C}) = 20.00(\pm 0.61) - 3.66(\pm 0.39) \times (\delta^{18}\text{O}_{\text{shell calcite VPDB}} - \delta^{18}\text{O}_{\text{water VSMOW}}), \quad (3)$$

240

241 Quoted errors on the slope and intercept are the 95 % confidence intervals. This equation was  
242 then used with the  $\delta^{18}\text{O}_{\text{shell calcite}}$  values of the six scallops to predict the temperature at which the  
243  $\text{CaCO}_3$  samples precipitated. The mean absolute error (MAE) shows the accuracy of the  
244 temperature prediction to be 1.0 °C.

245 The  $\delta^{18}\text{O}$ :temperature relationships calculated for each of the six shells are presented in  
246 Table 3. All relationships were highly significant ( $p < 0.001$ ), with  $r^2$  ranging from 0.490 to  
247 0.764, and MAE ranging from 0.8 to 1.2 °C. The test for comparison of slopes reveals that there  
248 is no significant difference between the slopes calculated (1) for each of the six shells ( $p =$   
249 0.447), (2) for the three shells of Sainte-Marie Bay ( $p = 0.589$ ), and (3) for three shells of  
250 Koutio Bay ( $p = 0.331$ ). Moreover, this test shows that the slope of the  $\delta^{18}\text{O}$ :temperature  
251 relationship is not significantly different for the two study sites ( $p = 0.127$ ). These results  
252 indicate that each specimen preserved similar information, a strong argument in support of the  
253 validity of this proxy.

254 The *C. radula*  $\delta^{18}\text{O}$ :temperature relationship predicts higher temperatures relative to  
255 estimates from paleotemperature equations commonly used over the range 20-30 °C (Fig. 5).  
256 Our  $\delta^{18}\text{O}_{\text{shell calcite}}$  data lie above the equilibrium line (as defined by the equation of Kim and  
257 O'Neil (1997) for  $[\text{HCO}_3^-] = 5 \text{ mM}$ ) by, on average, 0.73 ‰, equivalent to a temperature  
258 differential of about -3.6 °C. The slope of our equation compares favourably with the slopes of  
259 the relationships calibrated by Owen et al. (2002a) and Chauvaud et al. (2005) on the Great  
260 Scallop *Pecten maximus* (tests for comparison of slopes:  $p = 0.229$  and 0.903, respectively). It  
261 is, however, statistically different from the slope of Kim and O'Neil (1997) equation ( $p <$   
262 0.001).

263

264

## 4. DISCUSSION

265

### 4.1. Accuracy and limits of the temperature prediction

267

268 Using radioisotope measurements in the shell of the scallop, *Argopecten irradians*,  
269 Wheeler et al. (1975) found that the rate of mineral deposition was lower in the evening than at  
270 midday. Moreover, the timing of striae formation in this species was shown to be influenced by  
271 the photoperiod, with striae forming primarily in late afternoon and evening (Wrenn, 1972).  
272 Nothing is known about the timing of this process in *Comptopallium radula*. Although the time

273 resolution of our oxygen isotope analyses is high (each  $\delta^{18}\text{O}_{\text{shell calcite}}$  value represents an average  
274 of 4.6 days of  $\text{CaCO}_3$  precipitation), if calcification does not take place throughout the day then  
275 using average daily temperature values for the calibration of the equation can lead to errors as  
276 large as  $\pm 0.30$  °C in Sainte-Marie Bay and  $\pm 0.45$  °C in Koutio Bay. The sum of errors  
277 associated with the diurnal temperature amplitude, our 5-day averaging procedure, and the  
278 accuracy of the thermal probe ( $\pm 0.1$  °C), can explain nearly half (0.5 °C) of the 1.0 °C  
279 uncertainty of the temperature prediction. To proceed further with the use of isotopic signatures  
280 as environmental proxies, studies on the timing of  $\text{CaCO}_3$  deposition, in addition to better  
281 micro-analytical techniques at the scale of individual striae, are necessary.

282 It is also possible that the low sampling frequency for salinity (weekly measurements)  
283 was insufficient and induced an unknown amount of error. This is highlighted by a slightly  
284 greater mean absolute error for shells harvested from Koutio Bay, a site that experiences greater  
285 freshwater inputs and therefore more variable salinity (Table 3). Sea surface salinity (SSS) was  
286 measured from 1995 to 2003 at near-daily resolution close to Nouméa (ZoNeCo programme,  
287 “Variability of surface thermohaline structures in the New Caledonian Exclusive Economic  
288 Zone”). This dataset reveals occasional significant decreases in salinity (down to 28.9) on a sub-  
289 weekly basis following storms (characterized by large rainfall and elevated river runoff for 1 or  
290 2 days). If such salinity decreases occurred during our study, they may have been missed by our  
291 weekly sampling scheme, leading to errors in the estimation of the oxygen isotope composition  
292 of seawater used in the calibration equation.

293 A surprising result of our study is the weak influence of salinity on  $\delta^{18}\text{O}_{\text{shell calcite}}$  (Table 2).  
294 According to Eq. (2), salinity variations should generate annual ranges in  $\delta^{18}\text{O}_{\text{water}}$  of 0.24 to  
295 0.52 ‰ depending on the study site, which represents 14 to 30 % of the annual range in  
296  $\delta^{18}\text{O}_{\text{shell calcite}}$ . Therefore, it is astonishing that in our model salinity explains only 0.46 % of the  
297 variability of  $\delta^{18}\text{O}_{\text{shell calcite}}$ . The actual  $\delta^{18}\text{O}_{\text{water}}$ :salinity relationship, however, may be different  
298 from Eq. (2) if salinity variations at our study sites result from a balance between evaporation  
299 and precipitation rather than dilution by river water. Moreover,  $\delta^{18}\text{O}_{\text{water}}$ :salinity relationships

300 can be temporally variable on short timescales (Rohling and Bigg, 1998). Hence, the real annual  
301 range in  $\delta^{18}\text{O}_{\text{water}}$  may be different from the one calculated from Eq. (2). Temperature is, by far,  
302 the dominant factor controlling the shell oxygen isotope composition and this predominance, in  
303 addition to the existence of a significant effect of the "temperature\*salinity" interaction (Table  
304 2), may make it harder to identify the magnitude of a "salinity" effect. Nevertheless, we suggest  
305 that salinity-induced change in  $\delta^{18}\text{O}_{\text{water}}$  is not a major contributor to the  $\delta^{18}\text{O}_{\text{shell calcite}}$  record, as  
306 previously proposed by Quinn et al. (1996b) in their study on a massive coral from the  
307 southwest lagoon of New Caledonia.

308

#### 309 **4.2. Explanations for the observed fractionation**

310

311 Temperature reconstruction using molluscs is often considered straightforward by virtue  
312 of a longstanding assumption that the partitioning of oxygen isotopes between seawater and  
313 mollusc shells closely follows the isotopic equilibrium observed between inorganically  
314 precipitated calcium carbonate and water. Although this has been confirmed in a number of  
315 molluscs (Epstein et al., 1953; Kirby et al., 1998; Surge et al., 2001; Elliot et al., 2003), and in a  
316 scallop species (Chauvaud et al., 2005), other studies have reported disequilibrium precipitation  
317 of scallop shell calcite (Mitchell et al., 1994; Owen et al., 2002a,b). The variety of fractionation  
318 patterns observed implies that species-specific assessments must be completed. This is  
319 highlighted by the differences in the equations presented in Fig. 5. Discrepancies between  
320 mollusc records and their interpretations often arise from a lack of knowledge of the basic  
321 biology and ecology (growth rate, seasonal timing, and duration of growth) of the molluscan  
322 species used as environmental recorders.

323 We compared our  $\delta^{18}\text{O}_{\text{shell calcite}}$  values with those predicted by the Kim and O'Neil (1997)  
324 empirical equation, which is the most recent approximation for equilibrium partitioning of  
325 oxygen isotopes between inorganic calcite and seawater. Our results indicate that *C. radula*  
326 calcite is enriched in  $^{18}\text{O}$  by  $\sim 0.73\text{‰}$  with respect to inorganic calcite precipitated in  
327 equilibrium with water. Deviation from isotopic equilibrium in biogenic carbonates has been

328 explained historically in terms of “vital effects” (Urey, 1947) which include a combination of  
329 kinetic and metabolic effects (McConnaughey, 1989). Kinetic effects, inferred from a  
330 simultaneous depletion in  $^{18}\text{O}$  and  $^{13}\text{C}$  and a linear correlation between skeletal  $\delta^{18}\text{O}$  and  $\delta^{13}\text{C}$ ,  
331 have been observed at high calcification rates in the carbonate skeletons of some organisms  
332 (McConnaughey, 1989). A weak but statistically significant  $\delta^{18}\text{O}:\delta^{13}\text{C}$  linear relationship is  
333 observed when data from the 6 scallops are pooled ( $n = 225$ ,  $r^2 = 0.206$ ,  $p < 0.001$ ; Fig. 6).  
334 However, if kinetic effects associated with high *C. radula* calcification rates had occurred, we  
335 would have measured lower  $\delta^{18}\text{O}$  values than predicted by the Kim and O’Neil (1997) equation.  
336 In addition, no significant relationship was found between  $\delta^{18}\text{O}_{\text{shell calcite}}$  and shell growth rate  
337 (Table 2).

338 Kim and O’Neil (1997) observed that the extent of isotopic fractionation between water  
339 and calcite increased with increasing initial concentration of bicarbonate ions at any given  
340 temperature. They concluded that calcites precipitated from solutions of varying  $[\text{HCO}_3^-]$  were  
341 forming out of oxygen isotopic equilibrium with water since there should be only one  
342 equilibrium fractionation factor between calcite and water at any temperature. Spero et al.  
343 (1997) have shown that  $\delta^{13}\text{C}$  and  $\delta^{18}\text{O}$  values of calcitic shells of living planktonic foraminifera  
344 decrease as seawater  $[\text{CO}_3^{2-}]$  (or pH) increases. Zeebe (1999) suggested that the disequilibrium  
345 precipitation described by Kim and O’Neil (1997) may be explained by multiple equilibrium  
346 fractionations at a constant temperature but different pH values. Zeebe (1999) estimated that the  
347 pH of the solution resulting in the equation of Kim and O’Neil (1997) was 7.8 and that an  
348 increase in seawater pH by 0.1 unit produces a decrease of 0.11 ‰ in  $\delta^{18}\text{O}_{\text{calcium carbonate}}$ .

349 Two other recent studies found that the  $\delta^{18}\text{O}_{\text{shell calcite}}$  of the scallop *Pecten maximus*  
350 exhibited enrichment relative to equilibrium (as determined by the Kim and O’Neil (1997)  
351 equation) in both laboratory (+0.6 ‰; Owen et al., 2002a) and field experiments (+0.4 ‰;  
352 Owen et al., 2002b). Our observed +0.73 ‰ enrichment is in good agreement with results of  
353 these two studies. Using Zeebe’s model, the fractionation we measured in *C. radula* may be  
354 explained by a pH of ~7.14 in the extrapallial fluid (EPF) where shell calcification actually  
355 takes place. Analyses of marine bivalve EPF have shown its chemistry is significantly different

356 from that of seawater. The pH of EPF was measured in many marine bivalve species, with most  
357 values lying between 7.3 and 7.5, i.e., lower than in the external medium (for example, seawater  
358 at pH 7.9 to 8.2; Crenshaw, 1972; Wada and Fujinuki, 1976). This lowered pH is consistent  
359 with biomineralization models that assume the EPF is isolated from ambient seawater and that  
360 exchanges between this compartment and the external medium through the periostracum are  
361 limited, such as in the general model of molluscan shell calcification proposed by Wilbur and  
362 Saleuddin (1983). Therefore, the enrichment observed in the shell of *C. radula* could be related  
363 to low pH in the EPF compared to the pH in the experiment of Kim and O'Neil (1997), more  
364 than to vital effects.

365         According to Kim et al. (2006), however, Zeebe's model may be invalid and the isotopic  
366 fractionation between carbonate (aragonite and witherite) and water is independent of pH.  
367 Therefore, we suggest that the offset from equilibrium we observed may result from an isotopic  
368 signature of the EPF different from that of seawater, or by some kind of Rayleigh fractionation.  
369 The latter process occurs in a closed system or a finite reservoir when a chemical reaction  
370 fractionates isotopes and the reaction products are removed from the system or do not back-  
371 react. This results in a shift of the oxygen isotope composition of both the reactant and the  
372 product of the reaction. Rayleigh fractionation has been well described for changes in the  $\delta^{18}\text{O}$   
373 of water and vapour during evaporation where the vapour is continuously removed (i.e., isolated  
374 from the water) with a constant fractionation factor (Kendall and Caldwell, 1998). This process  
375 may occur during biocalcification of the shell of *C. radula* as (1) exchanges between the  
376 external medium and the extrapallial compartment are limited (semi-closed system; see Wilbur  
377 and Saleuddin, 1983), limiting the pool of  $\text{HCO}_3^-$  ions required by the reaction, and (2) the  
378 product of this reaction (i.e., calcite) does not back-react. If the effects of Rayleigh fractionation  
379 manifest themselves in the oxygen isotope system, they will result in  $^{18}\text{O}$  enrichment in both the  
380  $\text{HCO}_3^-$  reservoir and the precipitated calcite, as previously suggested by Mickler et al. (2004) to  
381 explain the offset from equilibrium they observed in modern tropical speleothems.

382

### 383 4.3. Conclusions

384

385 This study highlights the potential use of shells as high resolution archives of seawater  
386 temperature in New Caledonia. Our new  $\delta^{18}\text{O}$ :temperature relationship permits the  
387 reconstruction of seasonal SST variations within  $\pm 1.0$  °C over the temperature range 20-30 °C.  
388 Accuracy could be improved with better knowledge of the timing of striae formation and with  
389 salinity measurements at higher temporal resolution. We suggest that an observed 0.73 ‰ offset  
390 between the *C. radula*  $\delta^{18}\text{O}$ :temperature relationship and a recent equation describing isotopic  
391 equilibrium in inorganic calcite grown in seawater may be caused by (1) differences in solution  
392 pH between the scallop's extrapallial fluid and seawater, (2) an isotopic signature of the EPF  
393 different from that of seawater, or (3) Rayleigh fractionation in both the  $\text{HCO}_3^-$  reservoir and the  
394 calcite precipitated from it. These hypotheses remain to be demonstrated following detailed  
395 chemical analyses of the EPF.

396 In the past decade, several authors examined geochemical records ( $\delta^{18}\text{O}$ , Sr/Ca, Mg/Ca,  
397 U/Ca) of SST variability in corals from the tropical south west Pacific Ocean (e.g., Kilbourne et  
398 al. (2004) and references therein). These long-lived organisms can be used to reconstruct SST  
399 variations over several centuries. However, subannual SST reconstructions using corals are  
400 problematic because of the absence of clear sub-annual growth bands (Risk and Pearce, 1992).  
401 In most high resolution coral studies (e.g., Meibom et al., 2004), a chronology is developed by  
402 assuming constant growth rates and measuring distance along a transect, even though corals are  
403 known to exhibit highly variable daily growth rates (Risk and Pearce, 1992). In contrast, scallop  
404 shells can provide short SST time series (on the order of a few years) with very high temporal  
405 resolution (circa-daily), thus providing accurate estimates of the full range of environmental  
406 conditions that these organisms experience while growing. Scallops are thus more likely to  
407 record high frequency, extreme environmental events, at least as long as the stress induced does  
408 not interfere with the scallop's growth. This characteristic is particularly useful for the  
409 investigation of coral bleaching events. Moberg et al. (2005) pointed out the need for

410 multi-proxy approaches for accurate reconstruction of past seawater temperature variations, by  
411 combining long, low-frequency data sets (such as from corals) with high-frequency information  
412 (e.g., from scallop shell data). As a large edible species, ancient *C. radula* specimens are  
413 abundant at archaeological sites (J.-C. Galipaud, personal communication), and ancient shells  
414 may also be found by coring fossil reef or sand units. In this context, corals and scallops may  
415 become complementary tools for SST reconstructions in the tropical southwest Pacific.

416 *Acknowledgements.* We would like to express our gratitude to Sandrine Chifflet and Pierre  
417 Waigna (IRD New Caledonia) for their valuable help during the salinity: $\delta^{18}\text{O}_{\text{water}}$  calibration, as  
418 well as to Paul F. Dennis (University of East Anglia, England -  $\delta^{18}\text{O}_{\text{water}}$  analyses), and to  
419 François Michaud (Université de Bretagne Occidentale, France - XRD analyses). We would  
420 also like to acknowledge Alexandre Ganachaud and David Varillon (IRD New Caledonia) for  
421 providing us temperature and salinity data around Nouméa over the period 1995-2003 (ZoNeCo  
422 programme). Special thanks to Nolwenn Coïc for her help in maps and the production of  
423 figures. This manuscript has greatly benefited from critical reviews and very helpful comments  
424 by Alfonso Mucci, Donna Surge, Ann Goewert and two anonymous reviewers. This work was  
425 supported by IRD, the Programme National Environnement Côtier (PNEC) and the  
426 ACI-PECTEN. It was part of a 3-year research program funded by IRD and the Région  
427 Bretagne. Contribution N°1016 of the IUEM, European Institute for Marine Studies (Brest,  
428 France).

429

## REFERENCES

430

431 Andreasson F. P. and Schmitz B. (1996) Winter and summer temperatures of the early middle

432 Eocene of France from *Turritella*  $\delta^{18}\text{O}$  profiles. *Geology* **24**, 1067-1070.

433 Andreasson F. P. and Schmitz B. (1998) Tropical Atlantic seasonal dynamics in the early

434 middle Eocene from stable oxygen and carbon isotopes profiles of mollusk shells.

435 *Paleoceanography* **13**, 183-192.

436 Andreasson F. P. and Schmitz B. (2000) Temperature seasonality in the early middle Eocene

437 North Atlantic region: Evidence from stable isotope profiles of marine gastropod shells.

438 *Geol. Soc. Am. Bull.* **112**, 628-640.

439 Barbin V., Schein E., Roux M., Decrouez D. and Ramseyer K. (1991) Stries de croissance

440 révélées par cathodoluminescence dans la coquille de *Pecten maximus* (L.) récent de la

441 rade de Brest (Pectinidae, Bivalvia). *Geobios* **24**, 65-70.

442 Beck J. W., Edwards R. L., Ito E., Taylor F. W., Recy J., Rougerie F., Joannot P. and Henin C.

443 (1992) Sea-surface temperature from coral skeletal strontium/calcium ratios. *Science* **257**,

444 644-647.

445 Bice K. L., Arthur M. A. and Marincovich, Jr., L. (1996) Late Paleocene Arctic Ocean shallow-

446 marine temperatures from mollusc stable isotopes. *Paleoceanography* **11**, 241-249.

447 Chauvaud L., Thouzeau G. and Paulet Y.-M. (1998) Effects of environmental factors on the

448 daily growth rate of *Pecten maximus* juveniles in the Bay of Brest (France). *J. Exp. Mar.*

449 *Biol. Ecol.* **227**, 83-111.

450 Chauvaud L., Lorrain A., Dunbar R. B., Paulet Y.-M., Thouzeau G., Jean F., Guarini J.-M. and

451 Mucciarone D. (2005) Shell of the Great Scallop *Pecten maximus* as a high-frequency

452 archive of paleoenvironmental change. *Geochem. Geophys. Geosystems* **6**, Q08001.

453 doi:10.1029/2004GC000890.

454 Coplen T. B., Kendall C. and Hopple J. (1983) Comparison of stable isotope reference samples.

455 *Nature* **302**, 236-238.

- 456 Corrège T., Gagan M. K., Beck J. W., Burr G. S., Cabioch G. and Le Cornec F. (2004)  
457 Interdecadal variation in the extent of South Pacific tropical waters during the Younger  
458 Dryas event. *Nature* **428**, 927-929.
- 459 Craig H. (1965) The measurement of oxygen isotope paleotemperatures. In *Stable isotopes in*  
460 *oceanographic studies and paleotemperatures* (ed. E. Tongiorgi). Consiglio Nazionale  
461 delle Ricerche, Laboratorio di Geologia Nucleare, Pisa. pp. 161-182.
- 462 Craig H. and Gordon L. I. (1965) Deuterium and oxygen 18 variations in the ocean and marine  
463 atmosphere. In *Stable isotopes in oceanographic studies and paleotemperatures* (ed. E.  
464 Tongiorgi). Consiglio Nazionale delle Ricerche, Laboratorio di Geologia Nucleare, Pisa.  
465 pp. 9-130.
- 466 Crenshaw M. A. (1972) The inorganic composition of molluscan extrapallial fluid. *Biol. Bull.*  
467 **143**, 506-512.
- 468 Dunbar R. B. and Cole J. E. (1999) *Annual Records of Tropical Systems*. PAGES Workshop  
469 Report, Series 99-1, Bern, Switzerland.
- 470 Dutton A. L., Lohmann K. C. and Zinsmeister W. J. (2002) Stable isotope and minor element  
471 proxies for Eocene climate of Seymour Island, Antarctica. *Paleoceanography* **17**, 1016.  
472 doi:10.1029/2000PA000593.
- 473 Elliot M., deMenocal P. B., Linsley B. K. and Howe S. S. (2003) Environmental controls on the  
474 stable isotopic composition of *Mercenaria mercenaria*: Potential application to  
475 paleoenvironmental studies. *Geochem. Geophys. Geosystems* **4**, 1056.  
476 doi:10.1029/2002GC000425.
- 477 Epstein S. and Mayeda T. (1953) Variation of O<sup>18</sup> content of waters from natural sources.  
478 *Geochim. Cosmochim. Acta* **4**, 213-224.
- 479 Epstein S., Buchsbaum R., Lowenstam H. A. and Urey H. C. (1953) Revised carbonate-water  
480 isotopic temperature scale. *Bull. Geol. Soc. Am.* **64**, 1315-1326.
- 481 Gillikin D. P., Lorrain A., Navez J., Taylor J. W., André L., Keppens E., Baeyens W. and  
482 Dehairs F. (2005) Strong biological controls on Sr/Ca ratios in aragonitic marine bivalve  
483 shells. *Geochem. Geophys. Geosystems* **6**, Q05009. doi:10.1029/2004GC000874.

- 484 Hickson J. A., Johnson A. L. A., Heaton T. H. E. and Balson P. S. (2000) Late Holocene  
485 environment of the southern North Sea from the stable isotopic composition of Queen  
486 Scallop shells. *Palaeontol. Electronica* **3**, 1-11.
- 487 Kendall C. and Caldwell E. A. (1998) Chapter 2: Fundamentals of isotope geochemistry. In  
488 *Isotope tracers in catchment hydrology* (eds. C. Kendall and J. J. McDonnell). Elsevier  
489 Science B.V., Amsterdam. pp. 51-86.
- 490 Kennedy H., Richardson C. A., Duarte C. M. and Kennedy D. P. (2001) Oxygen and carbon  
491 stable isotopic profiles of the fan mussel, *Pinna nobilis*, and reconstruction of sea surface  
492 temperatures in the Mediterranean. *Mar. Biol.* **139**, 1115-1124.
- 493 Kilbourne K. H., Quinn T. M., Taylor F. W., Delcroix T. and Gouriou Y. (2004) El  
494 Niño-Southern Oscillation-related salinity variations recorded in the skeletal  
495 geochemistry of a *Porites* coral from Espiritu Santo, Vanuatu. *Paleoceanography* **19**,  
496 PA4002. doi:10.1029/2004PA001033.
- 497 Kim S.-T. and O'Neil J. R. (1997) Equilibrium and nonequilibrium oxygen isotope effects in  
498 synthetic carbonates. *Geochim. Cosmochim. Acta* **61**, 3461-3475.
- 499 Kim S.-T., Hillaire-Marcel C. and Mucci A. (2006) Mechanisms of equilibrium and kinetic  
500 oxygen isotope effects in synthetic aragonite at 25°C. *Geochim. Cosmochim. Acta.* **70**,  
501 A318.
- 502 Kirby M. X., Soniat T. M. and Spero H. J. (1998) Stable isotope sclerochronology of  
503 Pleistocene and Recent oyster shells (*Crassostrea virginica*). *Palaios* **13**, 560-569.
- 504 Krantz D. E., Jones D. S. and Williams D. F. (1984) Growth rates of the sea scallop,  
505 *Placopecten magellanicus*, determined from the <sup>18</sup>O/<sup>16</sup>O record in shell calcite. *Biol. Bull.*  
506 **167**, 186-199.
- 507 Krantz D. E., Williams D. F. and Jones D. S. (1987) Ecological and paleoenvironmental  
508 information using stable isotope profiles from living and fossil molluscs. *Palaeogeogr.*  
509 *Palaeoclimatol. Palaeoecol.* **58**, 249-266.

- 510 Lefort Y. (1994) Growth and mortality of the tropical scallops: *Annachlamys flabellata*  
511 (Bernardi), *Comptopallium radula* (Linne) and *Mimachlamys gloriosa* (Reeve) in  
512 southwest lagoon of New Caledonia. *J. Shellfish. Res.* **13**, 539-546.
- 513 Lefort Y. and Clavier J. (1994) Reproduction of *Annachlamys flabellata*, *Comptopallium radula*  
514 and *Mimachlamys gloriosa* (Mollusca: Pectinidae) in the south-west lagoon of New  
515 Caledonia. *Aquat. Living Resour.* **7**, 39-46.
- 516 McConnaughey T. (1989) <sup>13</sup>C and <sup>18</sup>O isotopic disequilibrium in biological carbonates: I.  
517 Patterns. *Geochim. Cosmochim. Acta* **53**, 151-162.
- 518 McCrea J. M. (1950) On the isotopic chemistry of carbonates and a paleotemperature scale. *J.*  
519 *Chem. Phys.* **18**, 849-857.
- 520 Meibom A., Cuif J.-P., Hillion F., Constantz B. R., Juillet-Leclerc A., Dauphin Y., Watanabe T.  
521 and Dunbar R. B. (2004) Distribution of magnesium in coral skeleton. *Geophys. Res. Lett.*  
522 **31**, L23306. doi:10.1029/2004GL021313.
- 523 Mickler P. J., Banner J. L., Stern L., Asmerom Y., Edwards R. L. and Ito E. (2004) Stable  
524 isotope variations in modern tropical speleothems: Evaluating equilibrium vs. kinetic  
525 isotope effects. *Geochim. Cosmochim. Acta* **68**, 4381-4393.
- 526 Mitchell L., Fallick A. E. and Curry G. B. (1994) Stable carbon and oxygen isotope  
527 compositions of mollusc shells from Britain and New Zealand. *Palaeogeogr.*  
528 *Palaeoclimatol. Palaeoecol.* **111**, 207-216.
- 529 Moberg A., Sonechkin D. M., Holmgren K., Datsenko N. M. and Karlén W. (2005) Highly  
530 variable Northern Hemisphere temperatures reconstructed from low- and high-resolution  
531 proxy data. *Nature* **433**, 613-617.
- 532 Owen R., Kennedy H. and Richardson C. (2002a) Experimental investigation into partitioning  
533 of stable isotopes between scallop (*Pecten maximus*) shell calcite and sea water.  
534 *Palaeogeogr. Palaeoclimatol. Palaeoecol.* **185**, 163-174.
- 535 Owen R., Kennedy H. and Richardson C. (2002b) Isotopic partitioning between scallop shell  
536 calcite and seawater: Effect of shell growth rate. *Geochim. Cosmochim. Acta* **66**, 1727-  
537 1737.

- 538 Pannella G. and MacClintock C. (1968) Biological and environmental rhythms reflected in  
539 molluscan shell growth. *J. Paleontol.* **42**, 64-80.
- 540 Quinn T. M. and Sampson D. E. (2002) A multiproxy approach to reconstructing sea surface  
541 conditions using coral skeleton geochemistry. *Paleoceanography* **17**, 1062.  
542 doi:10.1029/2000PA000528.
- 543 Quinn T. M., Crowley T. J. and Taylor F. W. (1996a) New stable isotope results from a  
544 173-year coral from Espiritu Santo, Vanuatu. *Geophys. Res. Lett.* **23**, 3413-3416.
- 545 Quinn T. M., Taylor F. W., Crowley T. J. and Link S. M. (1996b) Evaluation of sampling  
546 resolution in coral stable isotope records: A case study using records from New Caledonia  
547 and Tarawa. *Paleoceanography* **11**, 529-542.
- 548 Quinn T. M., Crowley T. J., Taylor F. W., Henin C., Joannot P. and Join Y. (1998) A  
549 multicentury stable isotope record from a New Caledonia coral: Interannual and decadal  
550 sea surface temperature variability in the southwest Pacific since 1657 A.D.  
551 *Paleoceanography* **13**, 412-426.
- 552 Risk M. J. and Pearce T. H. (1992) Interference imaging of daily growth bands in massive  
553 corals. *Nature* **358**, 572-573.
- 554 Rohling E. J. and Bigg G. R. (1998) Paleosalinity and  $\delta^{18}\text{O}$ : A critical assessment. *J. Geophys.*  
555 *Res. Oceans* **103**, 1307-1318.
- 556 Roux M., Schein E., Rio M., Davanzo F. and Filly A. (1990) Enregistrement des paramètres du  
557 milieu et des phases de croissance par les rapports  $^{18}\text{O}/^{16}\text{O}$  et  $^{13}\text{C}/^{12}\text{C}$  dans la coquille de  
558 *Pecten maximus* (Pectinidae, Bivalvia). *C.R. Acad. Sci. III* **310**, 385-390.
- 559 Sharp Z. D. (2006) *Principles of stable isotope geochemistry*. Prentice Hall, Upper Saddle  
560 River.
- 561 Spero H. J., Bijma J., Lea D. W. and Bemis B. E. (1997) Effect of seawater carbonate  
562 concentration on foraminiferal carbon and oxygen isotopes. *Nature* **390**, 497-500.
- 563 Surge D., Lohmann K. C. and Dettman D. L. (2001) Controls on isotopic chemistry of the  
564 American oyster, *Crassostrea virginica*: implications for growth patterns. *Palaeogeogr.*  
565 *Palaeoclimatol. Palaeoecol.* **172**, 283-296.

- 566 Tan F. C., Cai D. and Roddick D. L. (1988) Oxygen isotope studies on sea scallops,  
567 *Placopecten magellanicus*, from Browns Bank, Nova Scotia. *Can. J. Fish. Aquat. Sci.* **45**,  
568 1378-1386.
- 569 Thébault J., Chauvaud L., Clavier J., Fichez R. and Morize E. (2006) Evidence of a 2-day  
570 periodicity of striae formation in the tropical scallop *Comptopallium radula* using calcein  
571 marking. *Mar. Biol.* **149**, 257-267.
- 572 Tripathi A., Zachos J., Marincovich, Jr., L. and Bice K. (2001) Late Paleocene Arctic coastal  
573 climate inferred from molluscan stable and radiogenic isotope ratios. *Palaeogeogr.*  
574 *Palaeoclimatol. Palaeoecol.* **170**, 101-113.
- 575 Urey H. C. (1947) The thermodynamic properties of isotopic substances. *J. Chem. Soc.* 562-  
576 581.
- 577 Wada K. and Fujinuki T. (1976) Biomineralization in bivalve molluscs with emphasis on the  
578 chemical composition of the extrapallial fluid. In *The mechanisms of mineralization in the*  
579 *invertebrates and plants* (eds. N. Watabe and K. M. Wilbur). University of South  
580 Carolina Press, Columbia. pp. 175-190.
- 581 Watanabe T., Gagan M. K., Corrège T., Scott-Gagan H., Cowley J. and Hantoro W. S. (2003)  
582 Oxygen isotope systematics in *Diploastrea heliopora*: New coral archive of tropical  
583 paleoclimate. *Geochim. Cosmochim. Acta* **67**, 1349-1358.
- 584 Wheeler A. P., Blackwelder P. L. and Wilbur K. M. (1975) Shell growth in the scallop  
585 *Argopecten irradians*. I. Isotope incorporation with reference to diurnal growth. *Biol.*  
586 *Bull.* **148**, 472-482.
- 587 Wilbur K. M. and Saleuddin A. S. M. (1983) Shell formation. In *The Mollusca - Volume 4:*  
588 *Physiology - Part 1* (eds. A. S. M. Saleuddin and K. M. Wilbur). Academic Press, New  
589 York. pp. 235-287.
- 590 Wrenn S. L. (1972) Daily increment formation and synchronization in the shell of the bay  
591 scallop. *Am. Zool.* **12**, 32.
- 592 Zeebe R. E. (1999) An explanation of the effect of seawater carbonate concentration on  
593 foraminiferal oxygen isotopes. *Geochim. Cosmochim. Acta* **63**, 2001-2007.

## TABLES

Table 1. Summary of some previous  $\delta^{18}\text{O}$ :temperature relationships calibrated for inorganically precipitated calcite and for calcitic molluscs. Oxygen isotope compositions of calcite ( $\delta_c$ ) and water ( $\delta_w$ ) are expressed relative to VPDB and VSMOW, respectively.

Reference	Source	$t(^{\circ}\text{C}) = A + B (\delta_c - \delta_w) + C (\delta_c - \delta_w)^2$			Temperature range
		<i>A</i>	<i>B</i>	<i>C</i>	
Kim and O'Neil (1997) <sup>a</sup>	Inorganic	14.97	-4.97		10 - 40 °C
Owen et al. (2002a) <sup>a</sup>	Mollusc ( <i>Pecten maximus</i> )	17.15	-3.99		10 - 17 °C
Chauvaud et al. (2005)	Mollusc ( <i>Pecten maximus</i> )	14.84	-3.75		9 - 18 °C
Sharp (2006) <sup>b</sup>	Molluscs	15.75	-4.30	0.14	7 - 29.5 °C

(a) Rewritten in a form appropriate for comparison

(b) After Epstein et al. (1953) and Craig (1965)

Table 2. Multiple linear regression between *Comptopallium radula*  $\delta^{18}\text{O}_{\text{shell calcite}}$ , temperature, salinity, and shell growth rate in 2002-2003, considering or not shell growth rate.

	Estimate	Std. error	T	p
<i>Shell growth rate considered<sup>a</sup></i>				
<b>Intercept</b>	84.66	18.77	4.511	< 0.001
<b>Temperature (t)</b>	-3.200	0.733	-4.363	< 0.001
<b>Salinity (S)</b>	-2.241	0.527	-4.253	< 0.001
<b>Growth rate (GR)</b>	-0.016	0.017	-0.908	0.365
<b>t*S</b>	0.084	0.021	4.056	< 0.001
<b>t*GR</b>	0.0003	0.0001	2.193	0.029
<b>S*GR</b>	0.0003	0.0005	0.548	0.584
<i>Shell growth rate not considered<sup>b</sup></i>				
<b>Intercept</b>	77.98	18.45	4.227	< 0.001
<b>Temperature (t)</b>	-3.030	0.727	-4.170	< 0.001
<b>Salinity (S)</b>	-2.103	0.522	-4.027	< 0.001
<b>t*S</b>	0.081	0.021	3.937	< 0.001

(a) Multiple  $r^2$ : 0.705; adjusted  $r^2$ : 0.697; F-statistic: 86.68 on 6 and 218 DF;  $p$ -value: < 0.001.

(b) Multiple  $r^2$ : 0.694; adjusted  $r^2$ : 0.690; F-statistic: 166.8 on 3 and 221 DF;  $p$ -value: < 0.001.

Table 3. Parameters of the  $\delta^{18}\text{O}$ :temperature relationships (OLS regressions) calculated for each of the six shells separately, then for the shells of each study site separately. Also shown are the  $p$ -values resulting from the “comparison of regression lines” procedure.

Model fitting results: $t(^{\circ}\text{C}) = A + B (\delta^{18}\text{O}_{\text{shell calcite VPDB}} - \delta^{18}\text{O}_{\text{water VSMOW}})$							Test for equality of slopes			
Shell	$n$	$p$	$r^2$	$A$	$B$	MAE	Source	$p$	Source	$p$
SM1	38	< 0.001	0.748	19.45	-4.03	0.8	SM1	0.589	SM1	0.447
SM2	34	< 0.001	0.764	18.70	-4.04	0.8	SM2		SM2	
SM3	40	< 0.001	0.650	19.89	-3.53	0.8	SM3		SM3	
BK1	40	< 0.001	0.490	20.28	-3.86	1.2	BK1	0.331	BK1	
BK2	37	< 0.001	0.655	20.10	-3.73	0.9	BK2		BK2	
BK3	36	< 0.001	0.536	21.42	-2.88	1.0	BK3		BK3	
SM <sub>pooled</sub>	112	< 0.001	0.718	19.22	-3.95	0.8	SM <sub>pooled</sub>	0.127		
BK <sub>pooled</sub>	113	< 0.001	0.539	20.77	-3.37	1.1	BK <sub>pooled</sub>			

## FIGURE CAPTIONS

Fig. 1. a) Photograph of the upper surface of the left valve of *Comptopallium radula*. The maximal growth axis is indicated by the white arrow. b) Image (scanning electron microscopy) of striae taken along the maximal growth axis. These striae have been demonstrated to form with a 2-day periodicity (Thébault et al., 2006). Three shell samples drilled for isotopic analysis can be readily seen. Each sample contains material from two striae and is separated from the next one by two striae.

Fig. 2. Scallop sampling locations in the southwest lagoon of New Caledonia. Dashed line delimits the area of water sampling for  $\delta^{18}\text{O}_{\text{water}}$ :salinity calibration.

Fig. 3. Variations of  $\delta^{18}\text{O}_{\text{shell calcite}}$  (black points), bottom-water temperature (5-day moving average; black line) and shell growth rate (grey area) in the six studied *Comptopallium radula* specimens, from August 2002 to July 2003.

Fig. 4. Relationship between bottom-water temperature ( $^{\circ}\text{C}$ ) and  $(\delta^{18}\text{O}_{\text{shell calcite}} - \delta^{18}\text{O}_{\text{water}})$  where  $\delta^{18}\text{O}_{\text{shell calcite}}$  and  $\delta^{18}\text{O}_{\text{water}}$  are expressed on the VPDB and VSMOW scales, respectively. Also represented are the linear regression model and its equation.

Fig. 5. Comparison of temperature predictions using our new *Comptopallium radula*  $\delta^{18}\text{O}$ :temperature relationship and previously published paleotemperature equations. The position of our equation with respect to the theoretical equilibrium equation of Kim and O'Neil (1997) indicates that the shell of *Comptopallium radula* is not formed in isotopic equilibrium with seawater.

Fig. 6. Relationship between  $\delta^{18}\text{O}_{\text{shell calcite}}$  and  $\delta^{13}\text{C}_{\text{shell calcite}}$  of the 6 juvenile scallops (OLS regression:  $n = 225$ ,  $r^2 = 0.206$ ,  $p < 0.001$ ).

Figure 1

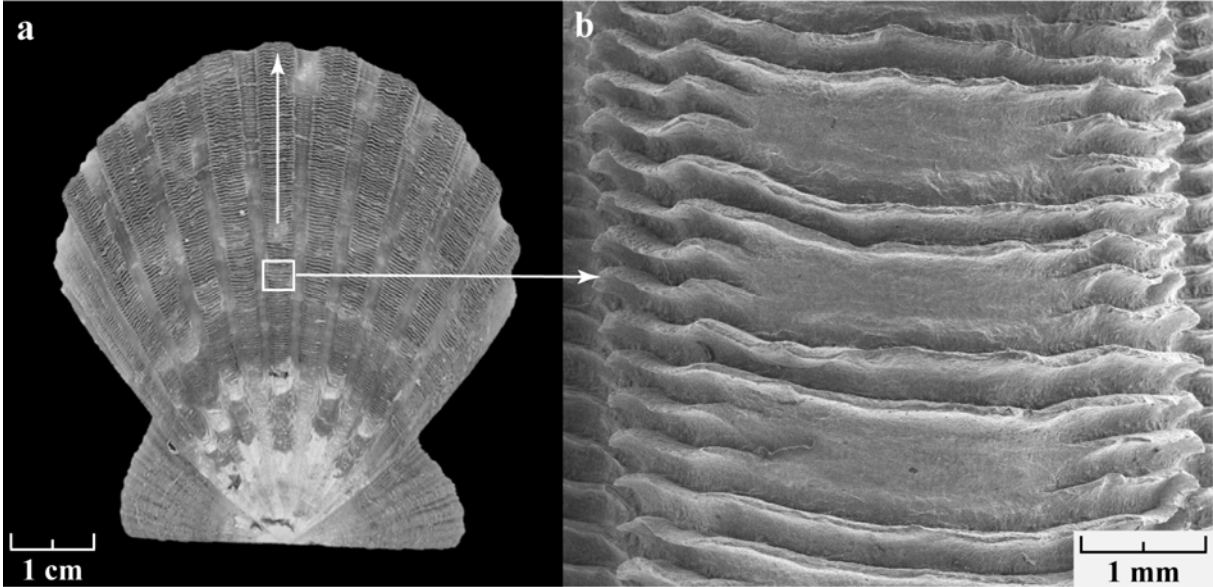
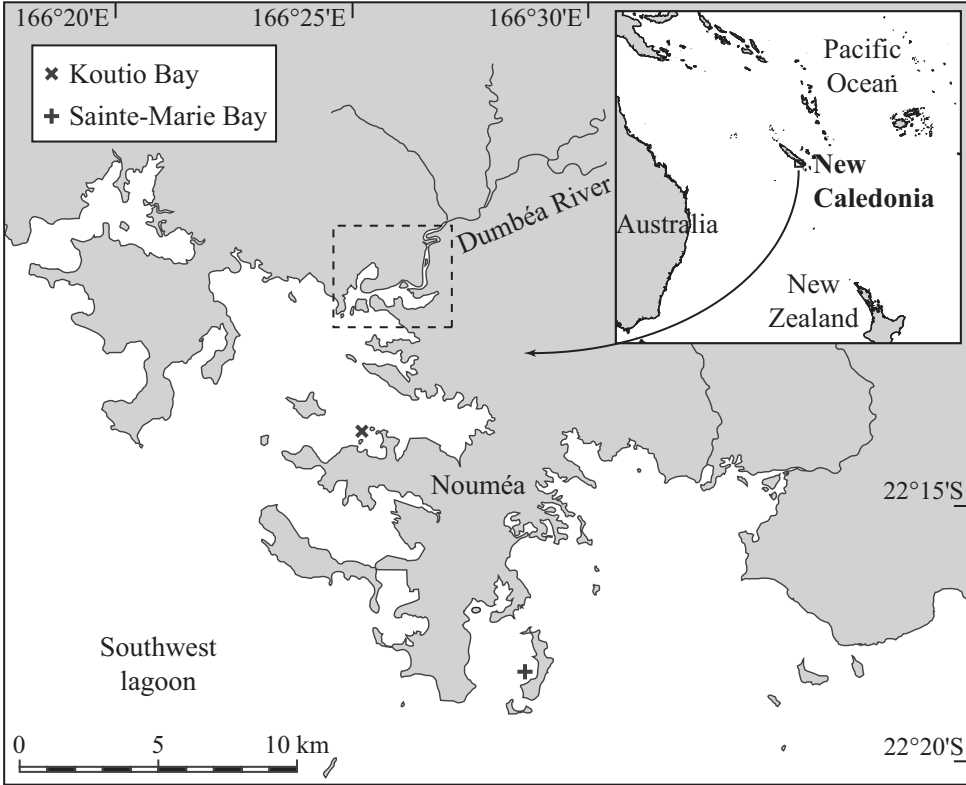


Figure 2



hal-00449317, version 1 - 21 Jan 2010

Figure 3

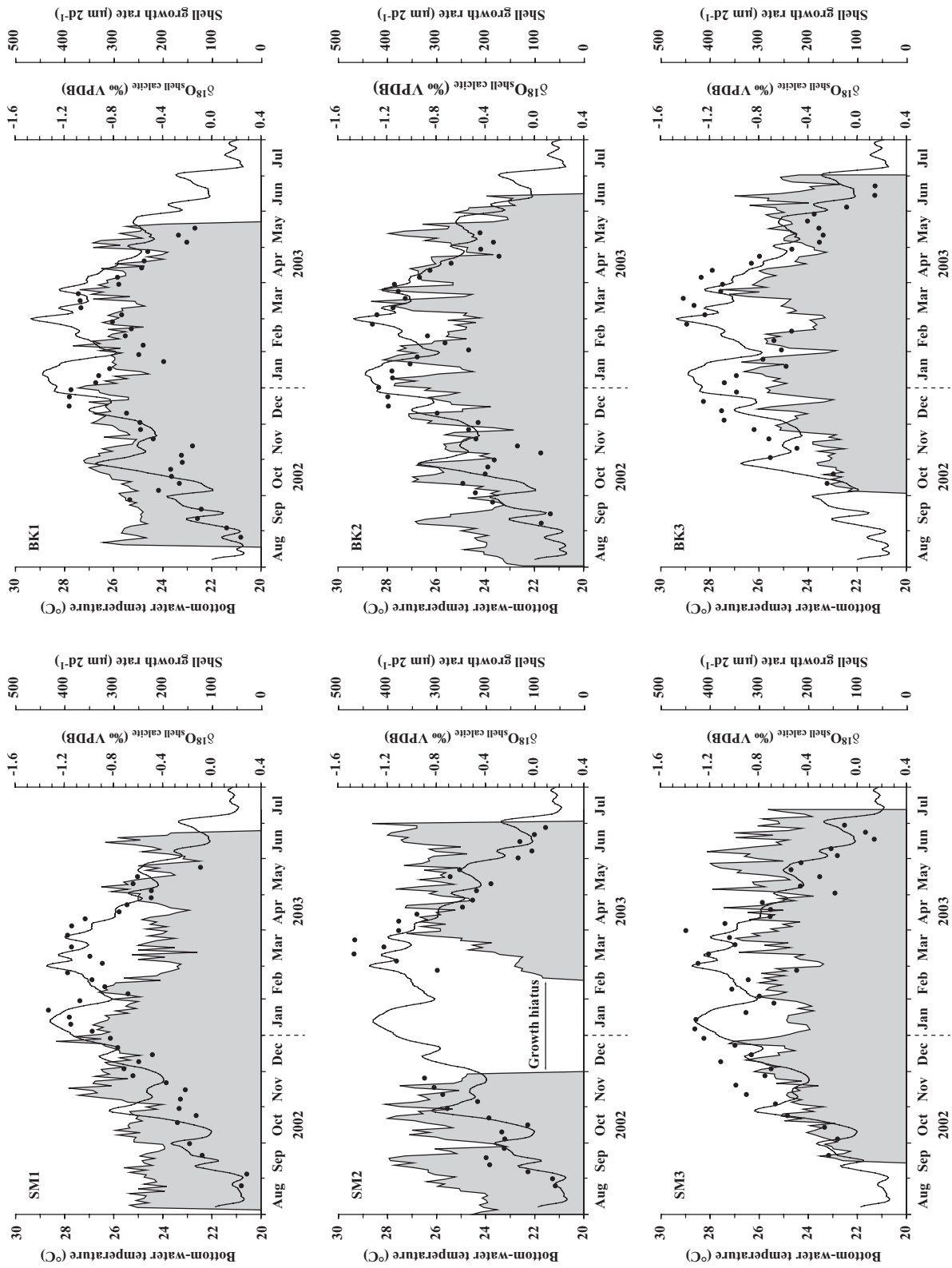


Figure 4

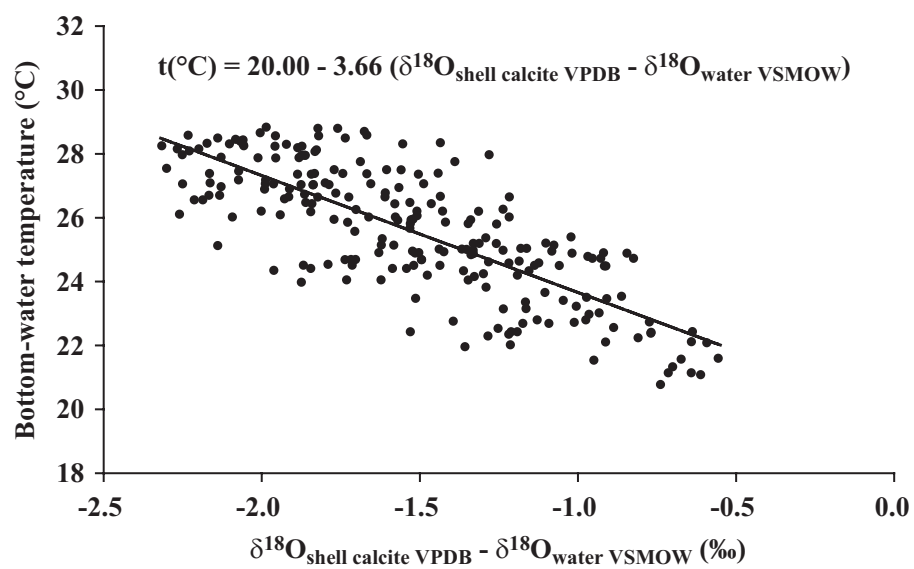


Figure 5

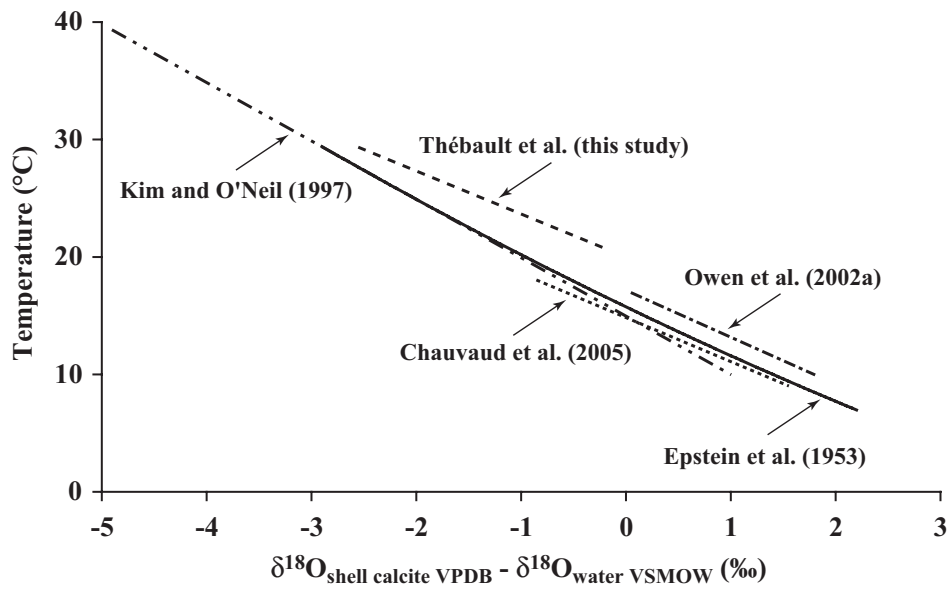


Figure 6

